JOURNAL OF MATERIALS SCIENCE 33 (1998) 4121–4129

Fatigue properties of jointed wood composites

Part II *Life prediction analysis for variable amplitude loading*

I. P. BOND, M. P. ANSELL
Department of Aerospace Engineering, University of Brisol, BS8 1TR, UK
School of Materials Science, University of Bath, BA2 7AY, UK

A method of predicting lifetime to failure for any wood composite system subjected to a complex load–time history has been developed. The prediction first requires the generation of a simple model to characterize the fatigue response of the particular composite system and a rainflow analysis breakdown of the load–time history under investigation. Once the models are derived they can be used to predict lifetimes to failure for any load–time history using a modified Palmgren–Miner damage summation rule. Variable amplitude fatigue testing of sample material using the same load–time histories allowed a comparison to be made between predicted and actual lifetimes to failure and was useful in verifying and refining the life prediction models.

1. Introduction

Fatigue has a major bearing on the design of any dynamically loaded structure. Traditionally, design against fatigue has been based on the performance of a material under constant amplitude fatigue conditions (cyclic stress application between two fixed values) at various R ratios (ratio of minimum stress, σ_{min}, to maximum stress σ_{max}) or on the basis of an estimated load spectrum using some form of damage accumulation rule, usually a derivative of the Palmgren–Miner rule. To date these have proved to be adequate techniques although they require a degree of conservatism to be incorporated into the design to account for the difficulty in predicting the effect of stochastic load conditions on the fatigue life of the material. One of the primary objectives of this work was, therefore, to develop a method for predicting more accurately the lifetime to failure of wood composite materials subjected to complex load–time histories driven by wind turbine blade research.

It is now widely accepted that constant amplitude loading insufficiently represents the interaction effects that occur in service loading, which is variable or stochastic in nature. Consequently, the best design against fatigue is unlikely to be produced because the available materials fatigue data are not truly representative of the loading in service.

Poppen and Bach [1, 2] have carried out extensive testing using *WISPER* and *WISPERX*. These are both standardized variable amplitude test loading sequences for use in fatigue evaluation of materials for horizontal axis wind turbine blades [3]. *WISPERX* is a filtered version of *WISPER* comprising only the most damaging cycles. It simulates the load conditions in the flapwise direction at a point close to the blade root. Fig. 1 shows the ε–N results of *WISPER* testing on [0°–±45°] glass–polyester. The line AO corresponds to life prediction using the Palmgren–Miner Rule ($D = \Sigma n_i/N_i$) [4] and Equations 1 and 2, which are used to obtain N_i instead of a constant life diagram. Equation 1 gives the number of cycles to failure, n_i, for stresses, σ_n, at different R ratios and was derived as a result of extensive analysis of published data by Appel and Olthoff [5].

$$\sigma_n = US(1 - D_m \log n) \tag{1}$$

$$D_m = 0.015A + 0.08 \tag{2}$$

where

$$A = 1 - R^* + R^* = \frac{\sigma_{min}/|\sigma_{min}|}{\sigma_{max}/|\sigma_{max}|} \tag{3}$$

where σ_{min} is the smallest absolute stress (or strain), σ_{max} is the largest absolute stress (or strain), σ_n is the individual stress (or strain) level, D_m is the damage parameter, US is either the ultimate tensile strength (UTS) or the ultimate compressive strength (UCS) depending on R ratio required, and n is the number of cycles.

The line BD corresponds to a life prediction based on curve fits to data from [1] resulting in Equation 4, a modified Equation 3.

$$D_m = 0.028A + 0.062$$

where

$$A = 1 - R^* + R^* = \frac{\sigma_{min}/|\sigma_{min}|}{\sigma_{max}/|\sigma_{max}|} \tag{4}$$

The prediction line AO is more conservative at higher strains than BD, which passes through the bulk of the

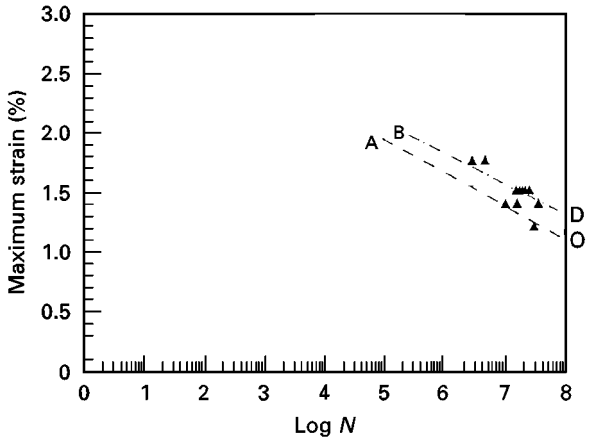

Figure 1 Results from *WISPER* tests on [0° ±45°] E-glass–polyester compared with two Palmgren–Miner rule-based life prediction models [1].

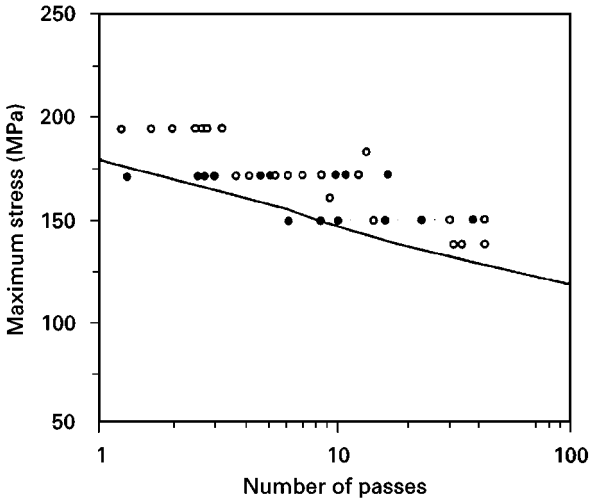

Figure 2 Results comparing *WISPER* (○) and *WISPERX* (●) tests on [±30°] E-glass–epoxy, including a Palmgren–Miner rule-based life prediction model [2].

experimental data but appears more optimistic at lower levels. This is to be expected because the life prediction curve AO is based on the Appel–Olthoff relationship which is conservative for $R = 0.1$ and *WISPER* is predominantly tensile.

Similar data to Fig. 1 is plotted in Fig. 2 for [±30°] E-glass–epoxy material. Only one life prediction model, based on the [0°–±45°] relation (Equation 1 and 2) and the Palmgren–Miner rule, is used to derive a curve. Again, the life prediction is conservative in relation to the actual test data. The differences in results obtained under *WISPER* and *WISPERX* are minimal. Generally, the scatter in the two data sets overlaps, with *WISPERX* perhaps showing slightly lower survival rates at comparable stress levels.

Three examples of the many possible methods for life prediction have been proposed by Liu and Lessard [6] for E-glass–epoxy composites. They are based on stiffness reduction, matrix crack density and size of delamination zone in the material. The stiffness reduction method is an obvious candidate for application to 'real' structural components as it is a parameter that can be easily measured. The matrix cracking and delamination size parameters are dependent on these forms of damage mechanisms being active during fatigue. In similar vein, O'Brien *et al.* [7] proposed a life prediction methodology for glass, carbon and hybrid–epoxy composites based on damage accumulation under tensile loading. Fatigue failure was predicted by comparing the changes in overall strain resulting from loss in stiffness when delaminations grow from matrix cracks spread throughout the laminate thickness.

Numerous other methods of life prediction for composite materials have been suggested. These include modulus degradation [8, 9], the derivation of a fatigue modulus [10], residual strength [11], the strength–life equal-rank–assumption [12, 13], cumulative damage [14] and energy criteria [15]. All have their strengths and weaknesses, but are generally most applicable to specific composite systems or to constant amplitude loading [16].

An extensive review of wood fatigue literature has been undertaken by Tsai [17] and supplemented by Bonfield [18]. Tsai reviewed literature dating as far back as the 1940s, most of which deals with the fatigue of wood in flexure, which reflects the traditional use of wood in civil engineering. More recently, during the 1980s, work in the USA on laminated wood–epoxy structures for wind turbine blades [19, 20] added to the limited amount of data available on wood composites under fatigue loading.

2. Experimental procedure

2.1. Derivation of life prediction models

Very little work has been done on the prediction of fatigue life for wooden structures. Previous work [18, 21] concerns the derivation of a life prediction model for assessing the life of a wood composite under complex loading. This model was empirically derived and its development first required the construction of a comprehensive constant life diagram requiring a large amount of static and fatigue coupon testing. The need to improve and optimize the method by which the dynamic behaviour of a composite material can be established was a driving force behind this work. A simplified method was required for developing composite-specific life prediction models, quickly and easily, which could then be used to predict fatigue performance of any new or modified material without the need for extensive re-testing.

Simple triangulated constant life diagrams can be constructed after minimal testing without great detriment to the fatigue performance envelope from *UTS*, *UCS* and reversed cyclic loading ($R = -1$) fatigue data [22]. These data can be obtained after relatively limited simple static and fatigue testing thus eliminating the need to characterize each new development of a composite system comprehensively.

The $R = -1$ fatigue data can be represented on either lin–log axes, where σ_{min} is plotted against log N, or log–log axes where log σ_{min} is plotted against log N. In both cases the median log N values at each

σ_{min} level tested are subjected to least squares regression analysis to give an equation (Equation 5) for 50% probability of failure. Section 4.2 discusses plotting the data.

$$\log N = \phi - m \times \sigma_{min} \text{ or } \log N = \phi - m \times \log \sigma_{min} \quad (5)$$

where ϕ and m are constants.

Starting with a simple, triangulated constant life diagram, a model for a particular composite can be rapidly derived. Values of mean stress, σ_m, and alternating stress, σ_a, for any R ratio can be obtained by constructing lines radiating from the origin and noting the point of intersection with the constant life lines. Fig. 3 depicts this for the four load conditions, tension–tension, tension–compression, compression–tension and compression–compression where a complete range of R ratios ($R = 0.9, 0.7, 0.5, 0.3, 0.1, -0.1, -0.3, -0.45, -0.6, -0.8, -1.5, -2, -3, -4, -6, 3, 5, 6, 8$ and 10) have been overlaid.

Plots can be made of the maximum stress, σ_{max} (means stress, σ_m, plus alternating stress, σ_a) at a point of intersection between an R ratio line and constant life line versus the value of the constant life line, to give a whole series of interpolated σ–N curves, Fig. 4. The gradient b, and intercept c, of all these interpolated σ–N curves can be obtained by linear regression to give a series of equations, like Equation 6, where the b and c values are required for derivation of the life prediction model.

$$\sigma_{max} = b \times \log N + c \quad (6)$$

Fatigue loading can be split into four load regimes, tension–tension (T–T), tension–compression (T–C), compression–tension (C–T) and compression–compression (C–C), which are represented by the following R and R'' ratio ranges. The R'' ratio is an arbitrary function used to provide sequential modes of cyclic loading.

$$\left.\begin{array}{lll} \text{T–T} & 0 < R < 1 \quad \& & 4 < R'' < 5 \\ \text{T–C} & -1 < R < 0 \quad \& & 3 < R'' < 4 \end{array}\right\}$$

where $R'' = 4 + R$

$$\left.\begin{array}{lll} \text{C–T} & -\infty < R < -1 \quad \& & 2 < R'' < 3 \\ \text{C–C} & 1 < R < \infty \quad \& & 1 < R'' < 2 \end{array}\right\}$$

where $R'' = 2 - 1/R$

If values of b and c calculated from interpolated σ–N curves using Equation 6 are plotted against their

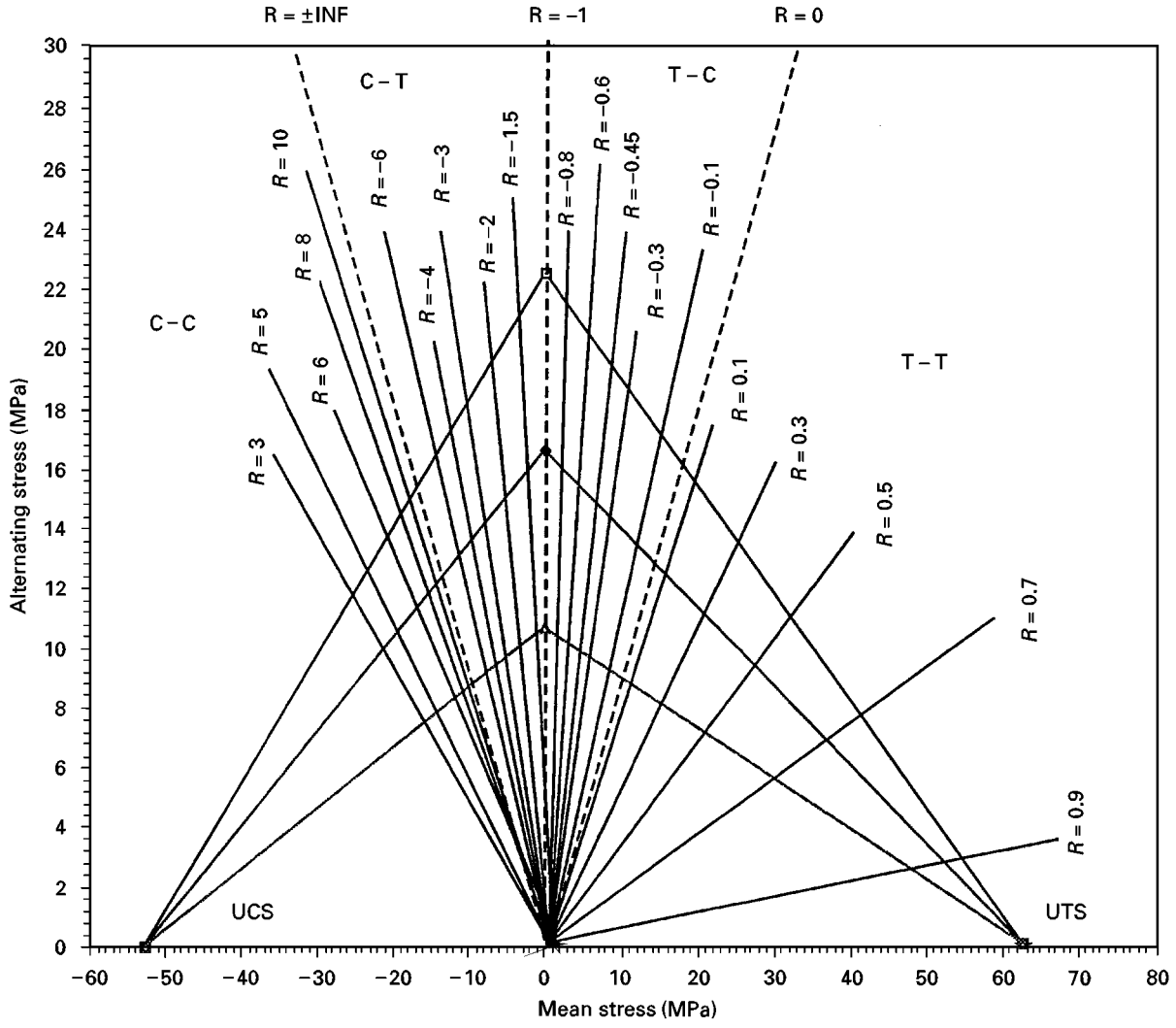

Figure 3 Intersection of constant life lines and R ratio lines. (–□–) 10^5, (–◆–) 10^6, (–△–) 10^7.

respective R'' value, quaternary polynomial relationships can be derived as

$$b = A \times (R'')^4 + B \times (R'')^3 + C \times (R'')^2 + D(R'') + E \quad (7)$$

$$c = P \times (R'')^4 + Q \times (R'')^3 + U \times (R'')^2 + V(R'') + W \quad (8)$$

These values of A B, C, D, E, P, Q, U, V and W are incorporated into a software package as an σ–N data set or *life prediction model*. The software requires the input of these b and c parameters to form a materials data set that subsequently allows the calculation of an σ–N curve for any R'' ratio (or R ratio) by their solution and substitution into Equation 6.

2.2. Life prediction model for a laminated wood composite

Examples of fatigue life prediction models derived from the experimental work presented in a preceeding paper [22] are shown below. The models are for a laminated poplar veneer composite that includes scarf joints in its structure. The models are based on static and reversed load ($R = -1$) fatigue data that have been plotted on both lin–log and log–log axes. All the models are derived from simplified constant life diagrams such as those described in Section 2.1 above. Equation 8 gives the life prediction, *model for scarf jointed poplar based on the lin–log* σ–N $R = -1$ *plot*

$$b = 0.731(R'')^4 - 8.708(R'')^3 + 37.336(R'')^2 - 68.356(R'') + 39.078$$

$$c = -3.266(R'')^4 + 39.396(R'')^3 - 164.170(R'')^2 + 276.520(R'') - 96.346$$

$$UTS = 62.58 \text{ MPa} \qquad UCS = -52.51 \text{ MPa} \quad (9)$$

Equation 9 gives the life prediction *model for scarf jointed poplar based on the log–log* σ–N $R = -1$ *plot*

$$b = 0.404(R'')^4 - 4.801(R'')^3 + 20.646(R'')^2 - 38.162(R'') + 21.960$$

$$c = -1.670(R'')^4 + 20.363(R'')^3 - 82.659(R'')^2 + 128.020(R'') - 11.735$$

$$UTS = 62.58 \text{ MPa} \qquad UCS = -52.51 \text{ MPa} \quad (10)$$

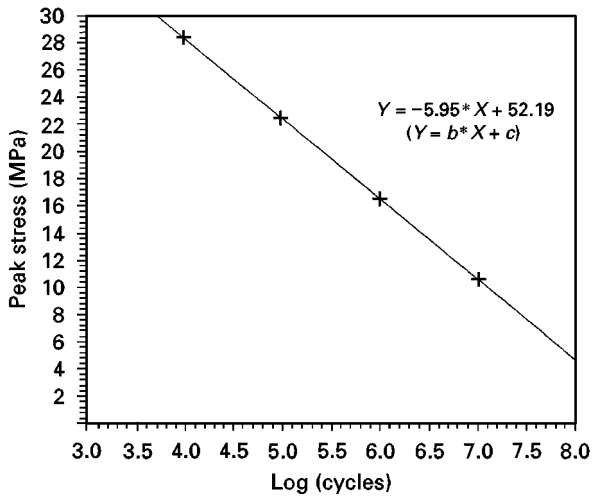

Figure 4 Plot of maximum stress, σ_{max}, versus log cycles to failure, log N, to derive $\sigma_{max} = b \times \log N + c$.

3. Life prediction for laminated wood composite materials: the WFA module

Collaboration with a commercial software company led to the further development of a fatigue analysis software package called WFA developed by Bonfield [18] in a previous research programme.

The WFA module functions by first "rainflow analysing" [3, 23] the load–time history under investigation to deconvolute the complex waveform into finite blocks of stress range, $\Delta\sigma$, and mean stress, σ_m, parameters. These are then counted and held in a 64×64 numerical matrix. The individual storage bins in this matrix correspond to the number of cycles at a particular R ratio and peak stress value. The number of cycles within each sector are summed and a distribution of the cycles within the waveform is produced. An example is shown in Fig. 5. For fatigue life prediction this histogram can be scaled using any factor, typically a proportion of the UTS or UCS.

The life prediction model described in Section 2.1 and 2.2 allows an σ–N curve to be interpolated for the material at any R ratio. A comparison is then made between the number of cycles for each R ratio in the waveform distribution histogram and the number of cycles to failure from the corresponding interpolated σ–N curve. This effectively provides a prediction of the amount of fatigue life lost to a single passage of the load–time history. Thus, using a simple damage

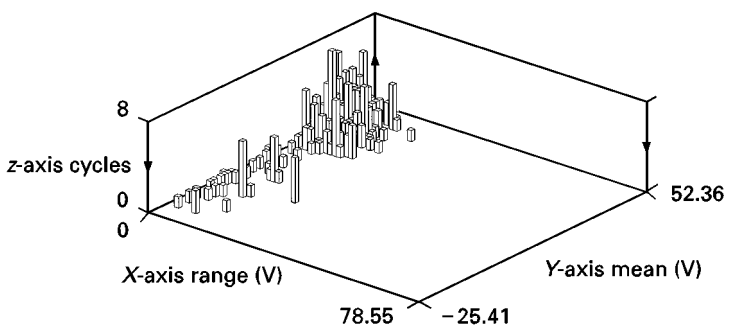

Figure 5 Cycle distribution histogram for the load–time history W9_4ES scaled to a proportion of the UTS.

accumulation rule, such as that derived by Palmgren–Miner, a prediction can be made as to the number of repetitions of the waveform the sample will survive under the conditions imposed. The load–time history and its scaling, the summation or D value used in the Palmgren–Miner relationship and the life prediction model can all be readily altered within the software.

4. Fatigue life prediction and variable amplitude testing

4.1. Complex load–time histories from instrumented blades in service.

The load cases used in this study were "real" load–time histories recorded from the blade of a 400 kW wind turbine generator. Three different 600 s campaigns were recorded under various conditions. After appropriate conditioning these waveforms were used to drive a servohydraulic test machine containing wood composite specimens. This effectively recreated the original variable amplitude loading in small coupons. Each short load sequence was repeated until failure of the sample. An example of one load–time history is shown in Fig. 6. The corresponding rainflow counted cycle distribution histogram is shown in Fig. 5.

4.2. Life prediction for scarf jointed poplar wood composites

As mentioned in Section 2.1, the different methods of plotting $R = -1$ fatigue data as either lin–log or log–log σ–N curves result in different interpolated values for allowable stress amplitudes, σ_a, at 10^4, 10^5, 10^6 and 10^7 cycles. This affects the form of the constant life diagram and thus ultimately the derived life prediction model. Table I compares the predictive abilities of life prediction models derived from $R = -1$ fatigue data plotted on lin–log and log–log axes. The load–time history is the same in both cases and is scaled according to proportions of the UTS and UCS. The model derived from the lin–log σ–N plot gives consistently higher predictions in both tension and compression than the log–log σ–N plot. It was found from comparison with the experimental results that life prediction models based on lin–log σ–N $R = -1$ plots were more accurate in predicting lifetime to failure.

TABLE I Comparison of life predictions $D = 1$, for W9_4ES using models derived from lin–log and log–log σ–N $R = -1$ data

% UTS or UCS for waveform peak	lin–log (No. of passes)		log–log (No. of passes)	
	Tensile	Compressive	Tensile	Compressive
50	21 134	129 000	6138	105 810
55	7009	45 756	990	19 336
60	2281	16 569	155	3656
65	743	5998	24	692
70	246	2172	3.9	131
75	80	786	<1	25
80	26	285	<1	4.7
85	8.5	103	<1	<1
90	2.8	37	<1	<1
95	<1	13	<1	<1

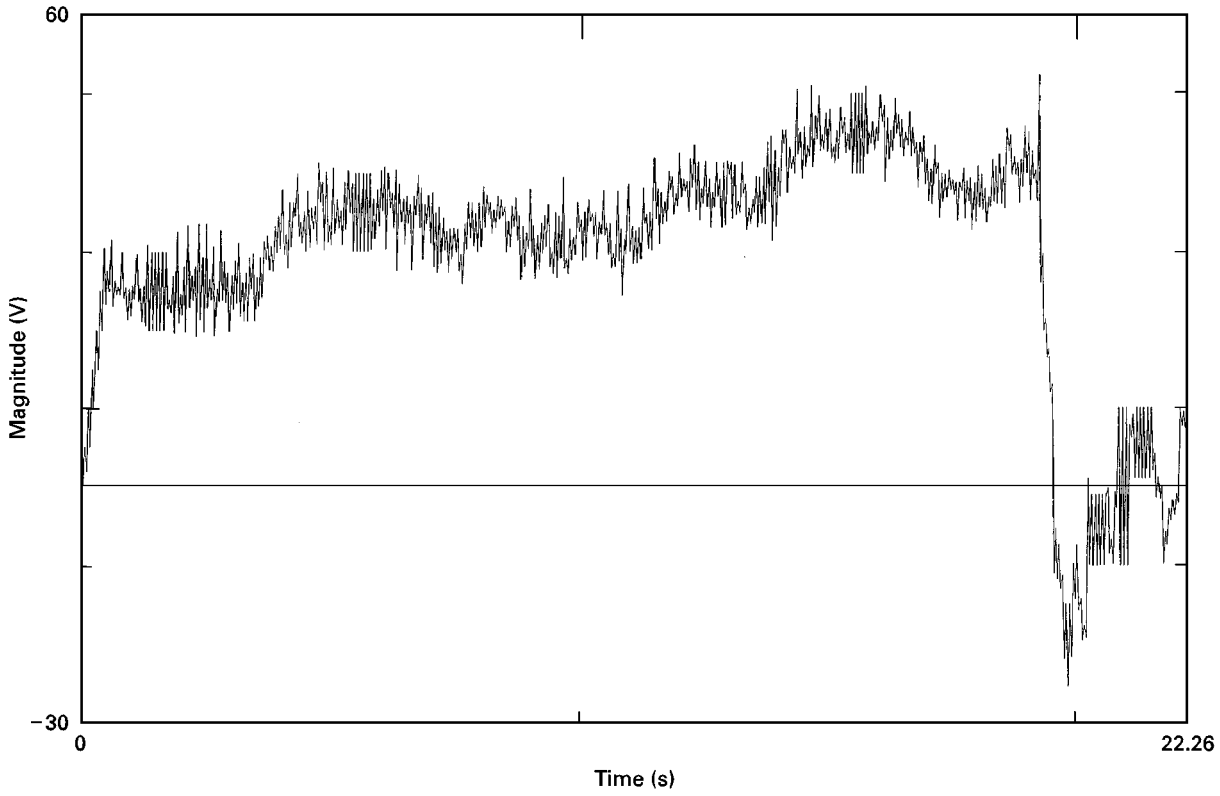

Figure 6 Complex load–time history W9_4ES: wind speed, 9.4 m s^{-1}; turbulence intensity, 15%; emergency stop sequence, 45 > 0 r.p.m.

Tables II and III are life predictions produced using the model shown in Equation 8 for different damage summation, D, values used in the Palmgren–Miner rule [4]. The results from only one of the three variable amplitude load–time histories for which the predictions were made are shown here. Comparing the tables it can be clearly seen that for the same life prediction model scaling as a proportion of the UTS results in a shorter predicted lifetime to failure than when scaled to the same percentage of the UCS.

The W9_4ES history is an emergency stop sequence that would occur extremely rarely. It has extreme transient loads (Fig. 5) with large stress range that have a very damaging effect. The R ratios that are predicted as being responsible for the majority of damage per single pass of W9_4ES lie within the mixed mode load regimes, tension–compression and compression–tension. They are also the cycles that have the largest stress range, $\Delta\sigma$, within the waveform. This corresponds to the findings of constant amplitude fatigue testing [22] where R ratios of mixed mode loading ($R = -1$, -0.84 and -3) showed markedly poorer fatigue performances than those of a single mode ($R = 0.33$ and $+3$).

Wind turbine rotor blades are designed to have a useful lifetime of 30 years. Each of the load–time histories used in the life prediction and testing were 10 min campaigns, which were assumed to be typical for the particular parameters that defined them. An extrapolation can therefore be made as to the number of repetitions per history that will add up to a 30 year life i.e. 1 580 000 repetitions. This is not very realistic as the loading conditions over this period will vary dramatically, from the rotor being stationary to it running under maximum loading. However, the prediction of allowable stresses for a 30 year life demonstrates the abilities of the life prediction model and gives an indication of the allowable stress level if the loading was always severe. The two load–time histories W9_4ES and W12_3S are both examples of stop sequences and thus will be seen by the blade only rarely, not repetitively as is assumed for the values in Table IV. As expected the steady state running condition history, W12_7P, allows appreciably higher peak stress levels than either of the two stop sequences.

TABLE II Life predictions for load–time history W9_4ES scaled to different percentages of the UTS of poplar

% UTS for wave form peak	Life prediction (No. of passes)			
	$D = 0.1$	$D = 1$	$D = 10$	$D = 100$
0.5	<1	21 134	211 340	2 113 400
0.55	<1	7009	70 090	700 900
0.6	<1	2281	22 811	228 110
0.65	<1	743	7425	74 250
0.7	<1	246	2463	24 631
0.75	<1	80	802	8020
0.8	<1	26	261	2612
0.85	<1	8.5	85	851
0.9	<1	2.8	28	277

TABLE III Life predictions for load–time history W9_4ES scaled to different percentages of the UCS of poplar

% UCS for wave form peak	Life prediction (No. of passes)			
	$D = 0.1$	$D = 1$	$D = 10$	$D = 100$
0.5	<1	129 000	1 290 000	12 900 000
0.55	<1	45 756	457 560	4 575 600
0.6	<1	16 569	165 690	1 656 900
0.65	<1	5998	59 980	599 800
0.7	<1	2172	21 716	217 160
0.75	<1	786	7862	78 620
0.8	<1	285	2847	28 468
0.85	<1	103	1031	10 307
0.9	<1	37	366	3656
0.95	<1	13	132	1322

TABLE IV Peak stress maxima for 30 year survival (1580 000 repetitions) of popular leminate subjected to each load–time history

Load–time history	Peak stress allowable for 30 year life (MPa)	Peak stress as a % of static strength	
		UTS	UCS
W9_4ES (tensile)	19.21	30.70	
W9_4ES (compressive	−19.24		37.60
W12_3S (tensile)	19.21	30.70	
W12_3S(compressive)	−19.95		38.00
W12_7P (tensile)	23.59	37.70	
W12_7P (compressive)	−23.79		45.30

4.3. Experimental procedure for fatigue testing

Experimental data was obtained by axial tension–compression testing of samples using a 200 kN Mayes servohydraulic test machine controlled by a DARTEC 9500 computer controller and fatigue data acquisition system. The test procedure required scaling of one of the load–time histories to percentages of the UTS or UCS of the wood under test. For testing scaled to the UCS the waveforms were inverted and the samples were held in an antibuckling device. Each specimen was then subjected to repeated passes of a waveform until failure occurred, the number of passes being recorded automatically. The rate of stress application was kept constant at 200 MPa s^{-1}. Five samples were tested at three different stress levels. The testing was carried out at relatively high percentages of UTS and UCS in order to reflect extreme load cases and to keep the test time to a practical level. Tensile and compressive loading was carried out to mimic the actual loading in the stressed skin blade structure where the pressure and suction side of the blade are predominantly tensile and compressive loading respectively. All test samples were dogbone shape and made from unidirectional laminated poplar of 4×5 mm layers, each layer incorporating a 7:1 scarf joint offset along the gauge length. Thin layers of $\pm 45^{\circ}$ glassepoxy were present on the two external surfaces of the samples [22].

5. Results and discussion

Experimental data points that correspond to the longevity of a sample when subjected to a *UTS* or *UCS* scaled waveform are overlaid onto life prediction curves obtained using a model specific to the poplar laminate. Prediction curves were produced with Palmgren–Miner damage summation values, *D*, of 0.1, 1, 10 and 100.

Fig. 7–11 show the correlation between theoretical life predictions and experimental data for scarf jointed poplar tested with the waveforms W9_4ES, W12_3S and W12_7P, scaled to the *UTS* (62.58 MPa) and *UCS* (−52.51 MPa), respectively.

In Fig. 7 the experimental data show little scatter and are centred around the prediction curve for $D = 100$, with the $D = 10$ curve acting effectively as a lower bound to the data. This implies that for the W9_4ES waveform the poplar life prediction model is heavily conservative, correlating to a Palmgren–Miner summation value two orders of magnitude larger than unity. In Fig. 8 the experimental data are spread between the $D = 1$ and $D = 10$ prediction curves. This reflects a greater accuracy in the model for the same waveform scaled in compression. The scatter of experimental data is small with few points falling outside these upper and lower prediction curves.

The results for waveform W12_3S scaled to the *UTS* are shown in Fig. 9. The prediction curve for $D = 10$ bisects the experimental data with the $D = 100$ and $D = 1$ predictions acting as upper and lower bounds. Two data points fall outside of the upper ($D = 100$) prediction curve but generally the scatter is not excessive. The predictive ability of the model correlates with the experimental data reasonably well exhibiting a slight conservative bias. When the same waveform is scaled to the *UCS* the resulting predictions change towards slight optimism, Fig. 10. The $D = 1$ curve intersects the experimental data, the majority of which lie between the $D = 10$ and $D = 0.1$ predictions. One experimental datum value at 85% *UCS* has given a notably low lifetime to failure and thus falls below the $D = 0.1$ curve. This was found to be a sample of poor quality manufacture that failed prematurely.

The results for the W12_7P waveform scaled to the *UTS* are shown in Fig. 11. This waveform represents steady state, continuous running conditions. The scatter in the experimental data is considerable, up to four orders of magnitude at 90% *UTS*, which means it is bounded by the highest, $D = 100$, and lowest, $D = 0.1$, predictions. The life prediction model could be construed as being slightly optimistic for this all tensile case, although the stress levels applied in order to

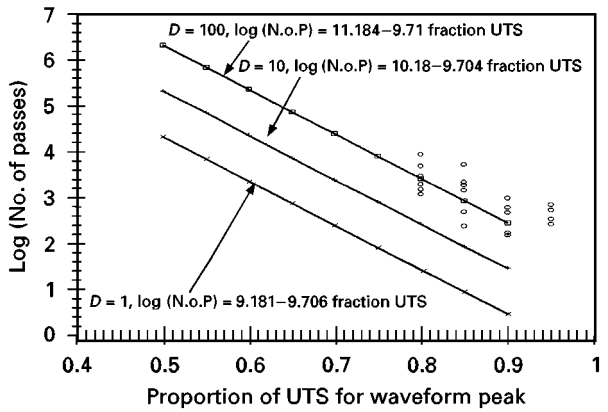

Figure 7 Life prediction ($D = 0.1$, 10 and 100) and experimental data (○) for scarf jointed poplar subjected to W9_4ES scaled to the *UTS*.

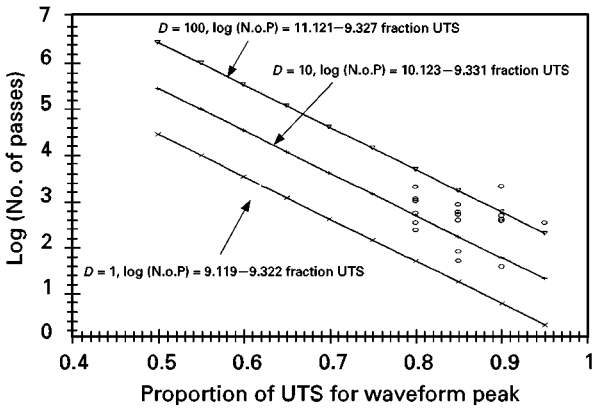

Figure 9 Life prediction ($D = 1$, 10 and 100) and experimental data (○) for scarf jointed poplar subjected to W12_3S scaled to the *UTS*.

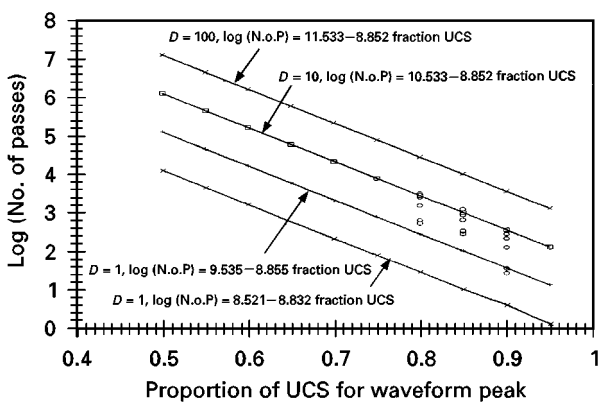

Figure 8 Life prediction ($D = 0.1$, 1, 10 and 100) and experimental data (○) for scarf jointed poplar subjected to W9_4ES scaled to the *UCS*.

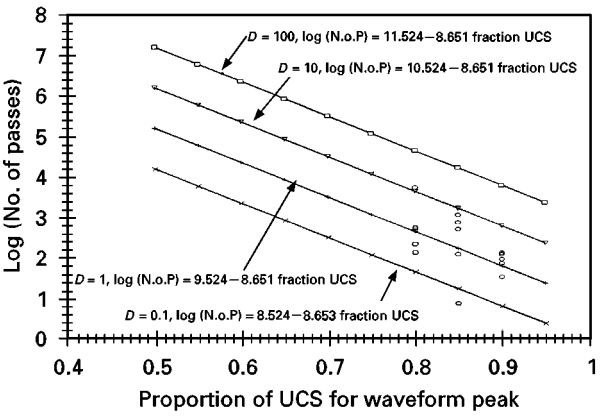

Figure 10 Life prediction ($D = 0.1$, 10 and 100) and experimental data (○) for scarf jointed poplar subjected to W12_3S scaled to the *UCS*.

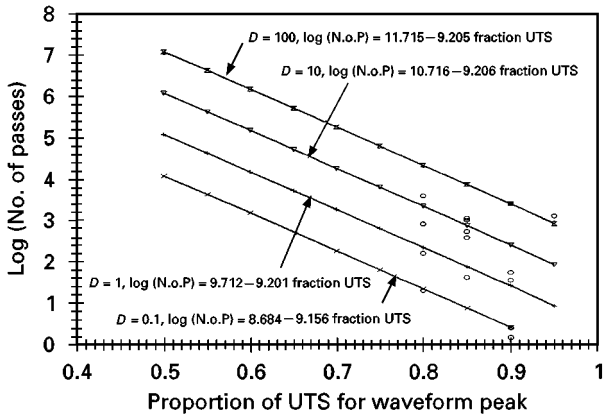

Figure 11 Life prediction ($D = 0.1$, 10 and 100) and experimental data (○) for scarf jointed poplar subjected to W12_7P scaled to the *UTS*.

achieve fatigue failure are higher than would be encountered in practice. No experimental data was obtained for the W12_7P waveform in compression so the model's predictive performance under all compressive loading has not been assessed.

For a given life prediction model and D value, the intercept and gradient of each prediction curve are functions of the waveform and life prediction model under investigation. They are a prediction by the respective life prediction models, of the rate of damage accumulation in the material when subjected to that load case.

The model is extremely conservative for the tensile W9_4ES loading (Fig. 7) requiring a D value of 100 to bisect the experimental data, but less so for the compressive case (Fig. 8), where a D value between 1 and 10 would divide the data. Likewise, for W12_3S, the experimental data in Fig. 9 would be bisected by a D value between 10 and 100 and in Fig. 10 by a D value of approximately 1. The poplar model exhibits a notable degree of conservatism when loading is mainly tensile and is a reasonably accurate predictor when loading is primarily compressive. This probably stems from the simple triangulated constant life diagrams on which the models are based. The implication from these results is that the act of simply linking static data points to fatigue data points at $R = -1$ excludes small but critical parts of the tension–tension and tension–compression performance envelopes (Fig. 3), which has a profound effect on the predictive accuracy of the subsequently derived life prediction model. Conversely, the compression–compression and compression–tension performance envelopes (Fig. 3) must be less susceptible to the loss of that parts as, in the examples shown here, the resulting life prediction model has a greater predictive accuracy under principally compressive loading.

Comparison of a comprehensive constant life diagram with a simple traingulated form and the effect on fatigue performance envelopes has been discussed in a previous paper [22]. The choice of a 50% survival probability regression curve in preference to a more conservative 95% condition when deriving the life prediction models reflects the principal aim of predicting experimental failure as accurately as possible.

Practical time constraints apply to all work on high cycle fatigue. This means that any empirical σ–N curve used in the derivation of a model will always be based on a limited amount of data, with possibly unforeseen consequences. Additionally, in the case of this life prediction methodology, the shortcomings in predictive accuracy are possibly compounded by the application of polynomial curve fitting, which could affect the model's sensitivity to different modes of loading.

Bonfield [18] and Bonfield and Ansell [21], in an earlier research programme, carried out variable amplitude testing and life prediction for unjointed wood laminates made from Khaya. Their original life prediction model was derived from a comprehensive constant life diagram obtained after extensive constant amplitude fatigue testing at several R ratios. The life predictions model was found to be conservative for predictions of predominantly tensile loading. These findings and the results of the research discussed above suggest that perhaps a load sequence effect occurs under complex variable amplitude loading that cannot be easily accounted for and thus incorporated into relatively simple life prediction models.

A degree of conservatism is often desirable in situations where failure is being predicted as it gives a safety margin and allows preventative measures to be taken if necessary. The method of predicting fatigue life discussed above has potential for application in the design of structures where little fatigue data are available and the service loading is likely to be varied. The empirical nature of Palmgren–Miner summation rule does not predetermine the values that D can take. A damage summation failure criterion ($\sum n_i/N_i = D$) where $D \neq 1$ has been shown, in this case, to improve predictive accuracy. Work by Poppen [24] on glass–epoxy composites subjected to a complex load–time history "*WISPER*" also found that a Palmgren–Miner value, D, not equal to unity was necessary to correlate experimental results with predictions from σ–N curves.

The prediction of exactly when and where damage occurs as a result of these load–time histories needs further investigation. However, it is clear that fatigue load sequences containing high mean and stress range combinations that occur suddenly within a load–time history are the most damaging to laminated wood composite materials. The bigger the range between highest tensile and lowest compressive excursion, the more damage is likely to result from each complex load–time history pass.

6. Conclusions

A method has been demonstrated by which life prediction models can be derived quickly and easily with a minimum of static and fatigue testing. Their basic requirement is static tensile and compressive data and fatigue data at one R ratio and subsequent derivation of two quaternary polynomials. Once derived they were used to predict lifetimes to failure using the Palmgren–Miner damage summation rule ($\sum n_i/N_i = D$) as a failure criterion.

Correlation with variable amplitude fatigue testing of coupon material using the same load–time sequences showed the models to have good predictive accuracy indicating a degree of conservatism under predominantly tensile loading but being more accurate under predominantly compressive loading. This is to be expected for systems based on wood that has a tensile strength higher than the compressive strength. Generally, the predictive abilities of the models are good considering the relatively little amount of data and the simple method on which they are based.

The use of a Palmgren–Miner damage summation rule with a value of $D \neq 1$ as a failure criterion improved the predictive accuracy in all load cases. This finding compares with those by other workers [21, 24] in that accurate life prediction for wood composites using similar methods requires D values not equal to unity.

Acknowledgements

The authors are very grateful to the UK Department of Trade and Industry for funding this work via the Energy Technology Support Unit under Contract No. W/44/00287 and the CEC DG-XVII for funding as a partner in the JOULE-II programme under Contract No. JOU2-CT92-0085.

References

1. POPPEN and P. W. BACH, *ECN Report*, ECN-RX--91-077 (The Netherlands Energy Research Foundation, Petten, The Netherlands, 1991).
2. R. MAYER (ed.), "*Fatigue properties and design of wing blades for wind turbines*" (Mechanical Engineering Publications, London, 1995).
3. A. A. TEN HAVE, Report No. NLR MP 87007U (National Aerospace Laboratory, Amsterdam, The Netherlands, 1987).
4. M. A. MINER, *Trans. ASME* **67** (1945) A159.
5. N. APPEL and J. OLTHOFF, *Polymarin Technical Report* (Polymarin B. V., Medemblik, The Netherlands, 1988).
6. B. Y. LIU and L. B. LESSARD, *Compos. Sci. Technol.* **51** (1994) 43.
7. T. K. O'BRIEN, M. RIGAMONTI and C. ZONOTTI, *Int J. Fatigue* **11** (1989) 379.
8. L. YE, *Compos. Sci Technol.* **36** (1989) 339.
9. L. J. LEE, J. N. YANG and D. Y. SHEU, *ibid.* **46** (1993) 21.
10. W. HWANG and K. S. HAN, *J. Compos. Mater.* **20** (1986) 154.
11. A. ROTEM, *Int. J. Fatigue* **10** (1988) 27.
12. P. C. CHOU and R. C. ROMAN, *J. Compos. Mater.* **12** (1978) 177.
13. P. M. BARNARD, R. J. BUTLERand P. T. CURTIS, *Int. J. Fatigue* **10** (1988) 171.
14. M. BENAMOZ, *Eng. Fract. Mech.* **37** (1990) 341.
15. V. KLIMAN, *Int. J. Fatigue* **7** (1985) 125.
16. B. HARRIS, N. GATHERCOLE, J. A. LEE, H. REITER and T. ADAM, *Phil. Trans. R. Soc. Lond. A* **355** (1997) 1259.
17. K. T. TSAI, PhD thesis, University of Bath, Bath (1987).
18. P. W. BONFIELD, PhD thesis, University of Bath, Bath (1991).
19. D. A. SPERA, J. B. ESGAR, M. GOUGEON and M. D. ZUTECK, "*Structural properties of laminated Douglas Fir–Epoxy composite material*" DOE/NASA/20320-76, NASA Reference Publication 1236, N91-10127 (US Department of Commerce, National Technical Information Service, Springfield, VA, 1990).
20. P. E. JOHNSON, "*Design of test specimens and procedures for generating material properties of Douglas Fir–Epoxy laminated wood composite material*", NASA-CR-174910, (US Department of Commerce, National Technical Information Service, Springfield, VA, 1985).
21. P. W. BONFIELD and M. P. ANSELL, *J. Mater. Sci.* **26** (1991) 4765.
22. I. P. BOND and M. P. ANSELL, *J. Mater. Sci.* **33** (1998) 2151.
23. M. P. ANSELL, in *Proceedings of the Seventh BWEA Wind Energy Conference – Wind Energy Conversion* 1987, edited by J. M. Galt (Mechanical Engineering Publications, London, 1987) pp. 39–54.
24. M. POPPEN, FFA Technical Report TN 1989–45 (Flygtekniska Försöksanstalten, The Aeronautical Research Institute of Sweden, Bromma, Sweden, 1989).

Received 24 September 1997
and accepted 11 May 1998